

30<sup>th</sup> Eurosensors Conference, EUROSENSORS 2016

## Torsional microresonator in the nonlinear regime: experimental, numerical and analytical characterization

Claudia Comi<sup>a</sup>, Alberto Corigliano<sup>a</sup>, Milena Doti<sup>a</sup>, Alessandro Garatti<sup>a</sup>, Giacomo Langfelder<sup>b</sup>, Valentina Zega<sup>a,\*</sup>

<sup>a</sup>Department of Civil and Environmental Engineering, Politecnico di Milano, piazza Leonardo da Vinci 32, Milano, 20133 Italy

<sup>b</sup>Department of Electronics, Information and Bioengineering, Politecnico di Milano, piazza Leonardo da Vinci 32, Milano, 20133 Italy

### Abstract

The dynamic behavior of a torsional microresonator is characterized analytically, numerically and experimentally both in the linear and nonlinear regime. Starting from the work presented in [1], here, the highly nonlinear regime is considered and the dynamic pull-in is experienced. Very good agreement between experimental data and numerical model is found also when the analytical methods usually employed to describe the nonlinear dynamic behavior of MEMS (multiple scale methods) are no more accurate. Finally, a numerical limit domain for the microresonator safe operation region in terms of bias and actuation voltages is computed and validated with experimental data.

© 2016 The Authors. Published by Elsevier Ltd. This is an open access article under the CC BY-NC-ND license

(<http://creativecommons.org/licenses/by-nc-nd/4.0/>).

Peer-review under responsibility of the organizing committee of the 30th Eurosensors Conference

**Keywords:** Torsional resonator; MEMS; nonlinearity; pull-in

### 1. Torsional resonator

Torsional resonators are largely used in MEMS and are of great interest because they can be employed as resonant components in inertial sensors (see for example the resonant accelerometer proposed in [2]) or as thermal sensors (see [3]) or as micromirrors (see [4]). Because of the wide range of application of this kind of device, it is crucial to be able to model the dynamic behavior also in the nonlinear regime.

The torsional resonator under study is fabricated through the Thelma<sup>©</sup> surface micromachining process developed by STMicroelectronics (see Figure 1a). It consists of a proof mass suspended by two folded torsional springs that allow a rotation  $\Theta$  around the  $a$ - $a$  axis; geometric dimensions of the device are reported in Table 1.

During its operation as resonator, the device is electrostatically actuated according to its first torsional mode by two electrodes located on the substrate under the proof mass (see Figure 1b): a time dependent voltage  $v_a(t)$  is applied to the driving electrode while the sensing electrode is grounded and the proof mass is kept to the bias voltage  $V_p$ .

Before starting with the analysis in the nonlinear regime, the quality factor  $Q$  of the resonator is experimentally evaluated for different bias voltages,  $V_p$ , and actuation voltages,  $v_a(t)$ , through the fitting of the linear frequency response (see Figure 2a). The values of  $Q$  thus obtained are shown by dots in Figure 2b, the variability is about 10%,

\* Valentina Zega. Tel.: +39-02-23994315 ; fax: +39-02-23994300.

E-mail address: [valentina.zega@polimi.it](mailto:valentina.zega@polimi.it)

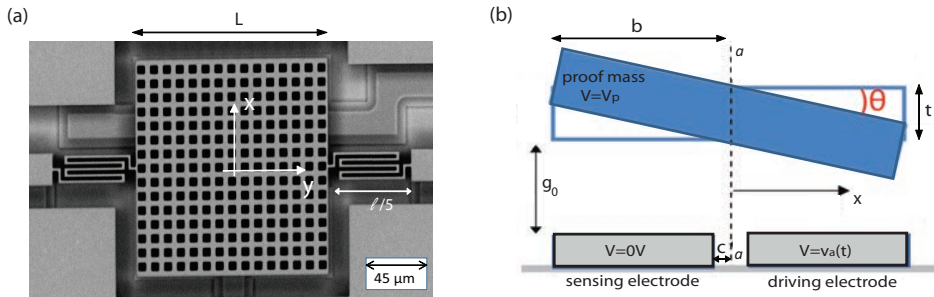


Fig. 1. (a) SEM image of the polysilicon torsional resonator fabricated through the Thelma<sup>©</sup> surface micromachining process developed by STMicroelectronics; (b) schematic view of the actuation scheme of the torsional resonator.

Table 1. Nominal values of the geometric parameters of the fabricated torsional resonator.

Parameter	Dimension	Parameter	Dimension
$L$	150 $\mu\text{m}$	$l$	247.7 $\mu\text{m}$
$b$	77.5 $\mu\text{m}$	$t$	24 $\mu\text{m}$
$c$	2 $\mu\text{m}$	$g_0$	1.8 $\mu\text{m}$

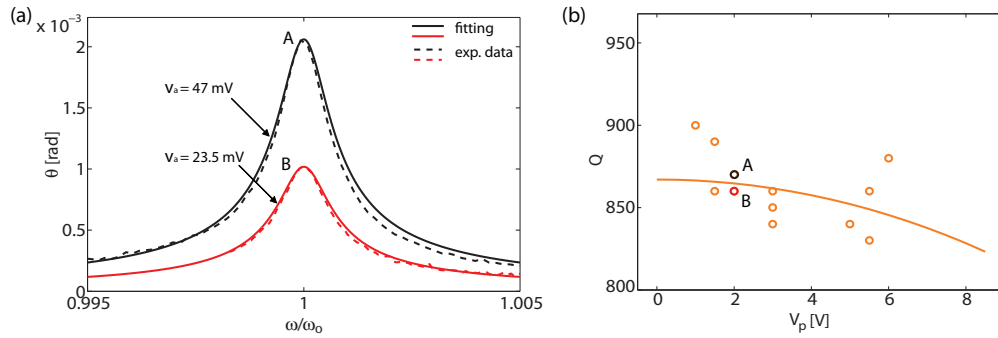


Fig. 2. (a) Experimental spectra and relative fitting curves for  $V_p=2\text{V}$  and  $|v_a|=23.5\text{ mV}$  and  $|v_a|=47\text{ mV}$  respectively; (b) Quality factor vs bias voltage: orange dots are obtained through fitting of the experimental linear frequency responses and the continuous line is the corresponding analytical prediction after identification of the damping coefficient.

in agreement with the instrument tolerance:  $Q$  values in this range are, then, used in the numerical and analytical models to predict the dynamic behavior of the device. The continuous curve in Figure 2b corresponds to the analytical prediction after identification of the damping coefficient.

### 2. Dynamic non-linear behavior of the torsional resonator

According to the actuation scheme shown in Figure 1b and under the one degree of freedom approximation of the torsional resonator, the equation of motion can be expressed as:

$$j\ddot{\Theta} + B\dot{\Theta} + K_m\Theta = T_e(t) \tag{1}$$

where

$$T_e = \int_c^b \left[ -\frac{1}{2} \frac{\epsilon_0 L}{(g_0 + \Theta x)^2} (V_p - v_a(t))^2 x \right] dx + \int_{-b}^{-c} \left[ -\frac{1}{2} \frac{\epsilon_0 L}{(g_0 + \Theta x)^2} V_p^2 x \right] dx \tag{2}$$

is the electrostatic moment acting on the resonator’s proof mass,  $j$  is the torsional inertia of the resonator,  $K_m = 2GJ_t/l$  is the torsional stiffness of the two folded springs,  $J_t$  is the torsional moment and  $B$  is the damping coefficient.

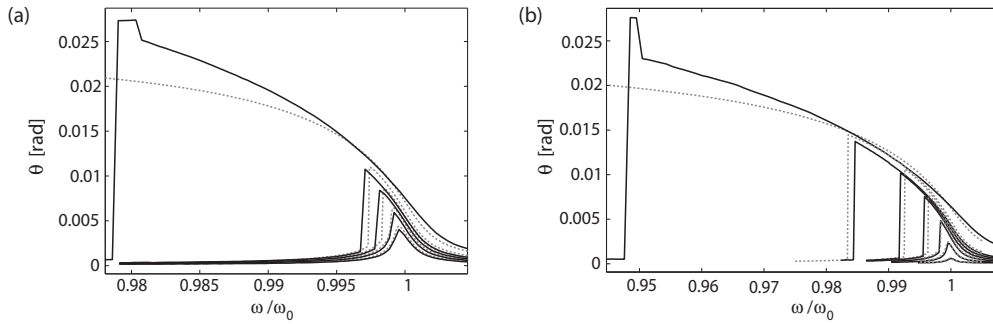


Fig. 3. Comparison between experimental data (continuous lines) and numerical predictions (dotted lines). Only the backward frequency sweeps are reported for sake of clarity. (a)  $V_p=4$  V and  $|v_a|=45, 65, 85, 105$  and  $150$  mV; (b)  $V_p=7$  V and  $|v_a|=3.5, 15, 30, 45, 60, 75$  and  $150$  mV.

Figures 3a and 3b show the experimental frequency responses obtained varying the actuation voltage,  $|v_a|$ , for  $V_p=4$ V and  $V_p=7$ V respectively, together with the numerical spectra computed solving the full dynamic equations of motion (1) through a 'brute-force' method. For low values of  $|v_a|$ , the usual linear frequency response is obtained. By increasing  $|v_a|$ , the hysteretic behavior is observed (note that in Figure 3 only the backward frequency sweep is shown for sake of clarity) till the occurrence of the dynamic pull-in. Note that while the numerical curve reaches an horizontal asymptote in proximity of the dynamic pull-in, the experimental curves experience a jump to the maximum physical admissible amplitude of the angle,  $\Theta_{max}$ . This discrepancy between experimental and numeric curves near the pull-in can be justified by the fact that, experimentally, it is not possible to reach asymptotically the  $\Theta_{max}$  value as adhesion forces, that are not taken into account in the model (1), arise in proximity of the contact between the resonator and the substrate. A very good agreement between the experimental data and the numerical prediction is, instead, observed far from the pull-in.

In order to show the importance of considering the full expression (2) of the electrostatic load, some analytical approximations of the frequency response of the torsional resonator are reported. The multiple scale method (see [5] for more details) is applied under the hypotheses  $V_p \gg |v_a|$  and  $|\Theta| = \theta \ll 1$  that allow the Taylor expansion of the electrostatic moment expression (2) with respect to  $\Theta$ . By taking into account only the first five terms of the Taylor expansion of (2), the frequency response of the resonator reads:

$$\left(\frac{\bar{T}_e}{k_1}\right)^2 = \left(2\left(1 - \frac{\omega}{\omega_0}\right)\theta + \frac{3k_3}{4k_1}\theta^3 + \frac{5k_5}{8k_1}\theta^5\right)^2 + \left(\frac{B}{j\omega_0}\theta\right)^2 \tag{3}$$

where  $\omega_0 = 2\pi f_0$  is the natural frequency of the resonator,  $k_1 = K_m - k_{e1}$  is the first order term of the stiffness and  $\bar{T}_e$ ,  $k_{e1}$ ,  $k_3$  and  $k_5$  are, respectively, the zero, first, third and fifth order terms of the Taylor expansion of (2).

In Figure 4 the experimental backward and forward frequency sweeps for  $V_p=5$ V and  $|v_a|=100$  mV are plotted together with the numerical and the first, third and fifth order analytical predictions obtained through the multiscale method. While the numerical model takes into account the full expression (2) of the nonlinear forcing term, the different analytical solutions, obtained from (3), consider the Taylor's expansion of the forcing term up to the first ( $k_3 = k_5 = 0$ ), third ( $k_5 = 0$ ) and fifth order, respectively. From Figure 4 is, then, evident that it is not possible to describe the real behavior of the torsional resonator, especially when the amplitude of rotation increases and the high non-linear regime is entered, with the analytical approximation (3). Even if the presence of the fifth order term in the Taylor expansion of the electrostatic moment (2) improves the commonly used third order 'Duffing approximation', the multiple scale method, because of its hypotheses, cannot be considered a tool able to follow the real non-linear behavior of a torsional resonator.

Finally, Figure 5 shows the limit pull-in domain, numerically obtained, of the torsional resonator under study in the  $V_p - |v_a|$  plane. Experimental frequency responses obtained for  $V_p - |v_a|$  combinations above the upper bound (orange points in Figure 5) show dynamic pull-in while for  $V_p - |v_a|$  combinations under the lower bound (black point in Figure 5), the classic linear or hysteretic behavior is obtained. The numerical lower bound, consequently, allows to define the safe operation region of the device.

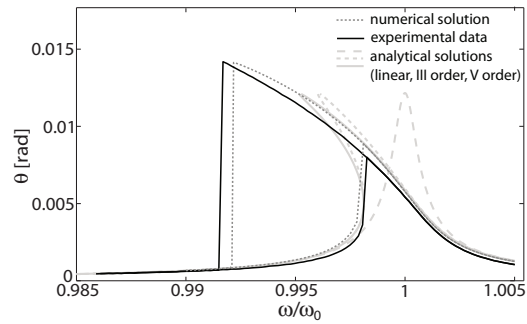


Fig. 4. Frequency response of the torsional resonator for  $V_p=5\text{V}$  and  $|v_a|=100\text{ mV}$ : linear, III and V order analytical approximations (gray curves), numerical prediction (dotted dark gray) and experimental curves (continuous black); both forward and backward frequency sweeps are shown.

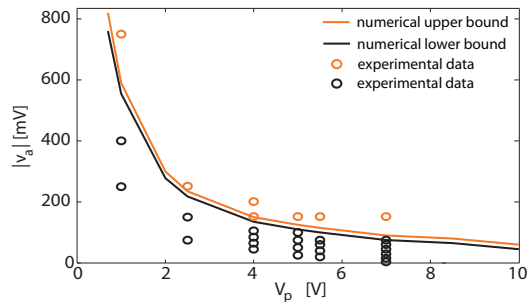


Fig. 5. Limit pull-in domain in the bias voltage-actuation voltage plane: numerical prediction (lines) and experimental measurements (dots). The couples of bias and actuation voltages leading to dynamic pull-in are shown in orange, while black corresponds to values of voltages leading to a dynamic response immune to pull-in.

### 3. Conclusions

In this paper the dynamic behavior of the torsional resonator has been deeply studied also in the nonlinear regime. The inadequacy of analytical methods based on strict hypotheses on the amplitude of the oscillation angle, to describe the nonlinear behavior of a MEMS resonator is proved together with the suitability of numerical methods.

A limit pull-in domain is shown and the good agreement between theoretical predictions with the experimental data demonstrates that it is possible to predict in a very accurate way the safe region where the resonator can operate without any instability problems.

Note that all the proposed considerations can be extended to other devices whose dynamic response is governed by the equation of motion (1) and can enter the highly nonlinear regime during their operation.

### Acknowledgements

ST-Microelectronics<sup>©</sup> is gratefully acknowledged by the authors for the fabrication of the studied device.

### References

- [1] A. Caspani, C. Comi, A. Corigliano, G. Langfelder, V. Zega, S. Zerbini, Dynamic Nonlinear Behavior of Torsional Resonators in MEMS, *J. of Micromech. and Microeng.* 24 (2014) 1–9.
- [2] C. Comi, A. Corigliano, G. Langfelder, V. Zega, S. Zerbini, Sensitivity and temperature behavior of a novel z-axis differential resonant micro accelerometer, *J. of Micromech. and Microeng.* 26 (2016) 1–11.
- [3] X. C. Zhang, E. B. Myers, J. E. Sader, M. L. Roukes, Nanomechanical Torsional Resonators for Frequency-Shift Infrared Thermal Sensing, *Nano Lett.* 13(4) (2013) 1528–1534.
- [4] V. Milanovic, M. Last, K. S. J. Pister, Torsional micromirrors with lateral actuators, *Transducers 01*, Muenchen, Germany, Jun. 2001.
- [5] A. H. Nayfeh and D. T. Mook, *Nonlinear Oscillations*, Wiley Classics Library Edition Published.